Macromolecules **2008**, *41*, 4321−4327

Conductive Polymer Functionalization by Click Chemistry

Anders Egede Daugaard and Søren Hvilsted*

Danish Polymer Centre, Department of Chemical and Biochemical Engineering, Technical University of Denmark, Building 423 Produktionstorvet, DK-2800 Kgs. Lyngby, Denmark

Thomas Steen Hansen and Niels B. Larsen

Polymer Department, POL-313, P.O. Box 49, Frederiksborgvej 399, DK-4000 Roskilde, Denmark

Received December 7, 2007; Revised Manuscript Received April 21, 2008

ABSTRACT: Click chemistry is used to obtain new conductive polymer films based on poly(3,4-ethylenedioxythiophene) (PEDOT) from a new azide functional monomer. Postpolymerization, 1,3-dipolar cycloadditions in DMF, using a catalyst system of $CuSO_4$ and sodium ascorbate, and different alkynes are performed to functionalize films of PEDOT-N_3 and copolymers prepared from EDOT-N_3 and 3,4-ethylenedioxythiophene (EDOT). This approach enables new functionalities on PEDOT that could otherwise not withstand the polymerization conditions. Reactions on the thin polymer films have been optimized using an alkynated fluorophore, with reaction times of ~20 h. The applicability of the method is illustrated by coupling of two other alkynes: a short chain fluorocarbon and a MPEG 5000 to the conductive polymer; this alters the advancing water contact angle of the surface by +20° and −20°/−25°, respectively. The targeted chemical surface modifications have been verified by X-ray photoelectron spectroscopy analysis.

Introduction

Conductive polymers have been extensively studied during the past few decades for applications such as biosensors,[1] strain gauges,[2] organic solar cells,[3] or organic light-emitting diodes.[4] Many challenges have to be met in the development of new functional conducting polymers, including synthesis of monomers with the required functionality and establishment of polymerization conditions compatible with the targeted function. Specific problems may be instability of large biological molecules for biosensors under the typically harsh polymerization conditions or inhibition of the polymerization process by a side reaction with a functional group in the monomer. Functionalization of the conductive polymer may result either from incorporation of the functional entity into the monomer during monomer synthesis or by postpolymerization coupling of the targeted functionality to built-in generic coupling sites in the monomer unit. Recently, the term "click chemistry" was defined by Sharpless et al.[5] as selection criteria for highly efficient coupling reactions. Ideally, the click reaction can be performed in water or organic solvents at room temperature, making the method suitable for most applications. Click chemistry has mainly been based on the use of 1,3-dipolar cycloadditions of azides and alkynes under copper catalysis[6,7] and Diels−Alder reactions. In polymer chemistry it has been used in numerous ways e.g. for end-group functionalization,[8] polymer to polymer couplings,[9] functionalization of linear polymers with selected groups,[10] dendrons,[11] and poly(ethylene glycol) (PEG).[12] Also, in reactions on surfaces the cycloaddition has been used with good results e.g. to bond metal surfaces together.[13] It has been used with carbon nanotubes[14] and for functionalization of self-assembled monolayers on gold.[15,16] Recently click chemistry has also been used for surface reactions on cotton[17] and glass.[18,19] A bioactive surface has been prepared by introduction of biotin by click chemistry on a polymer substrate.[20] For sensor applications especially biological systems are of great interest, and these often require mild reaction conditions, which can be obtained using click chemistry.[21] A comprehensive review on macromolecular click chemistry has recently been published by Binder et al.[22]

The new developed conducting polymer is based on PEDOT, used in numerous applications due to its high electrical conductivity and high stability in ambient and aqueous environments.[23] During polymerization the polymer becomes insoluble, and further functionalization becomes difficult. Combination of the conductive properties of PEDOT and the advantages of modularity, high selectivity, and high yields of click chemistry permits preparation of new PEDOTs for many different applications, e.g., surfaces with conductive properties or sensors. Both pre- and postfunctionalization have been studied by others. With regards to biological active molecules the most successful methods so far is physical absorption after polymerization or entrapment during polymerization.[24] Covalent postfunctionalization has been achieved through peptide bonding.[25,26] The click approach is a good alternative that gives a controlled functionalization without protective groups through high selectivity. In our group we have focused on the use of PEDOT for different applications[27−30] and the use of click chemistry for polymer functionalization.[31] Here we present a standardized method for postpolymerization functionalization of PEDOT to obtain conductive polymer surfaces with various functionalities.

Experimental Section

General Methods. Thin layer chromatography (TLC) was performed on Merck plates coated with silica gel F254. Kieselgel for column chromatography was Merck Kieselgel 60 (230−400 mesh). ^{1}H NMR was run on a 250 MHz cryomagnet from Spectrospin and Brucker at room temperature. Infrared spectroscopy (IR) was performed on a Perkin-Elmer Spectrum One model 2000 Fourier transform infrared system with a universal attenuated total reflection sampling accessory on a ZnSe/diamond composite. Differential scanning calorimetry (DSC) was performed on a DSCQ1000 from TA Instruments. The thermal analyses were performed at a heating and cooling rate of 10 °C/min. The melting temperatures (T_m) are reported as the peak temperatures of the endothermic melting peaks. The conductivity was measured with a four-point probe (Jandel Engineering Ltd., Linslade, UK) connected to a four-point source meter (Keithley 2400, Cleveland, OH). Film thicknesses were measured with an Ambios XP-2 (Ambios

---

* Corresponding author. E-mail: sh@kt.dtu.dk.

10.1021/ma702731k CCC: $40.75

Technology, Inc., Santa Cruz, CA) profilometer using a stylus force of 0.5 mg. Optical microscopy images was recorded with a AxioCam MRc 5 camera mounted on a Zeiss Axioskop 40 microscope (Oberkochen, Germany). Fluorescence analysis was conducted with a Zeiss Filter Set 09 (excitation 450−490 nm, emission >515 nm). XPS analysis was performed on a Thermo Fisher Scientific K Alpha (East Grinstead, UK) using monochromatized aluminum Kα radiation in a 400 μm spot on the sample. Survey and high-resolution spectra were acquired and analyzed using the manufacturer's Avantage software package. Spectra were generally acquired with electron charge compensation in operation to avoid sample charging, except for a series of measurements to determine the detrimental effects of electron flooding on azide functional gruops. Atomic force microscopy analysis proceeded on a PSIA XE-150 instrument operating in intermittent contact mode with BudgetSensor Tap-300 cantilevers.

Chemicals. Chemicals except for Baytron C were acquired from Aldrich and were used as received unless otherwise specified. Baytron C was purchased from H.C. Starck. Fluorescein methyl ester was prepared in accordance with Moore et al.[32]

3,4-(1-Bromomethylethylene)dioxythiophene, 1 (EDOT-Br). 3,4-Dimethoxythiophene (0.41 g, 2.8 mmol), 3-bromo-1,2-propanediol (1.11 g, 7.2 mmol), and *p*-toluenesulfonic acid (0.08 g, 0.4 mmol) were dissolved in toluene (30 mL) and stirred at 100 °C for 48 h. Toluene was removed in vacuo, and the residue was dissolved in CH_2Cl_2 and extracted with Na_2CO_3 and H_2O. The organic phase was dried with $MgSO_4$, filtered, and concentrated in vacuo, and the crude product was purified by column chromatography with a gradient eluent of heptane/ethyl acetate (EtOAc). The product was isolated as a colorless oil (0.24 g, 37%). IR (cm^{-1}): 3112 (C−H stretch). ^1H NMR ($CDCl_3$, 250 MHz, δ_H, ppm): 3.4−3.6 (m, 2H, $CH_2{-}Br$); 4−4.44 (m, 3H, $O{-}CH_2{-}CH{-}O$); 6.36/6.37 (2 × d, ^4J = 3.7 Hz, 2H, S−CH).

3,4-(1-Azidomethylethylene)dioxythiophene, 2 (EDOT-N_3). 1 (0.22 g, 0.9 mmol) and NaN_3 (0.08 g, 1.2 mmol) were dissolved in DMF (10 mL) and stirred at room temperature (RT) for 17 h. The reaction mixture was diluted with H_2O (15 mL), and the aqueous DMF was extracted with EtOAc (5 × 15 mL). The organics were combined and extracted with H_2O (3 × 15 mL) and brine (1 × 15 mL), dried with $MgSO_4$, filtered, and concentrated in vacuo to give the product as a colorless oil (0.18 g, 97%). IR (cm^{-1}): 3114 (C−H stretch); 2097 ($-N_3$ stretch). ^1H NMR ($CDCl_3$, 250 MHz, δ_H, ppm): 3.4−3.6 (m, 2H, $CH_2{-}N_3$); 4−4.44 (m, 3H, $O{-}CH_2{-}CH{-}O$); 6.36/6.39 (2 × d, ^4J = 3.7 Hz, 2H, S−CH).

General Polymerization Method for 2, to PEDOT-N_3, 3. The polymerization method was based on an earlier published method for the polymerization of EDOT.[33] A number of microscope slides were thoroughly cleaned using acetone, isopropanol, ethanol, and water. The glass slides were surface modified by vapor phase hexamethyldisilazane (HMDS) in a dedicated oven (Yield Engineering Systems 6112). **2** (20 mg,0.15 mmol), Baytron C (0.48 mL, ~40 wt % Fe(III)Tos in butanol), and butanol (0.48 mL) were mixed and spin-coated on the glass-slides (10 s at 1000 rpm). The samples were placed on a hot plate at 65 °C for 5 min and subsequently washed with water and blown dry in a nitrogen flow, yielding films with a thickness of 200−250 nm.

General Copolymerization Method for Poly(3,4-ethylenedioxythiophene-*co*-3,4-(1-azidomethylethylene)dioxythiophene). The copolymerization method was based on an earlier published method for the polymerization of EDOT.[33] A solution of 3,4-ethylenedioxythiophene (EDOT, 0.22 mL), Baytron C (6.5 mL), butanol (6.5 mL), and pyridine (0.15 mL) was mixed with the EDOT-N_3 solution mentioned above to yield solutions containing 5 (**4**), 10 (**5**), 20 (**6**), 40 (**7**), 60 (**8**), and 80 mol % (**9**) EDOT-N_3 of the total monomer content. The polymerization mixtures were then spin-coated onto the HDMS treated glass slides (10 s at 1000 rpm). The samples were placed on a hot plate at 65 °C for 5 min and subsequently washed with water and blown dry in a nitrogen flow.

General Ester Synthesis, 2,2,3,3,3-Pentafluoropropyl Pent-4-ynoate, 10. A solution of 4-pentynoic acid (0.60 g, 6.1 mmol), dimethylaminopyridine (DMAP, 0.12 g, 0.9 mmol), and 2,2,3,3,3-pentafluoropropanol (0.97 g, 6.5 mmol) in CH_2Cl_2 (15 mL) was stirred at RT, and a solution of *N,N′*-dicyclohexylcarbodiimide (DCC, 1.58 g, 7.6 mmol) in CH_2Cl_2 was added dropwise. The reaction mixture was stirred overnight at RT, filtered, and concentrated in vacuo. The crude product was purified by column chromatography using a gradient eluent of pentane/ether and gave a colorless oil (1.24 g, 88%). IR (cm^{-1}): 3314 ($C{\equiv}C{-}H$ stretch); 2119 ($C{\equiv}C$ stretch); 1761 ($O{-}C{=}O$ stretch); 1197, 1143, 1107 (C−F stretch). ^1H NMR ($CDCl_3$, 250 MHz, δ_H, ppm): 1.99 (t, ^4J = 2.6 Hz, 1H, $H{-}C{\equiv}$); 2.54 (m, 2H, ${\equiv}C{-}CH_2{-}$); 2.67 (m, 2H, $-CH_2{-}COO{-}$); 4.57 (tq, ^4J = 1 Hz, ^3J = 12.9 Hz, 2H, $O{-}CH_2{-}CF_2$).

Methyl 2-(3-Oxo-6-(prop-2-ynyloxy)xanthen-9-yl)benzoate, 11. Fluorescein methyl ester (2.00 g, 5.8 mmol), triphenylphosphine (TPP, 4.55 g, 17.3 mmol), and propargyl alcohol (0.98 g, 17.5 mmol) were stirred in acetonitrile/THF (50/50) at 0 °C. Diethylazodicarboxylate (DEAD, 3 mL, 17.3 mmol) was added slowly, and the mixture was stirred overnight at RT. The crude mixture was poured onto a Kieselgel column and chromatographed using an eluent of 80/20 CH_2Cl_2/ether, followed by a gradient of CH_2Cl_2/EtOAC. The product was collected from the top of the column with EtOAc as a yellow crystalline compound (1.08 g, 49%, T_m = 206 °C). IR (cm^{-1}): 3193 ($-C{\equiv}C{-}H$ stretch); 2123 ($C{\equiv}C$ stretch); 1729 ($O{-}C{=}O$ stretch). ^1H NMR ($CDCl_3$, 250 MHz, δ_H, ppm): 3.59 (s, 3H, O-CH3); 5.00 (s, 2H, ${\equiv}C{-}CH_2{-}O$); 6.26 (s, 1H, Ar−H); 6.40 (m, 1H, Ar−H); 6.7−7.0 (m, 3H, Ar−H); 7.28 (s, 1H, Ar−H); 7.50 (m, 1H, Ar−H); 7.7−8.0 (m, 2H, Ar−H); 8.21 (s, 1H, Ar−H).

α-Methoxypoly(ethylene glycol)-ω-pent-4-ynoate, 12. The product was prepared according to the general procedure for ester synthesis by DCC coupling, using a commercially available methoxypoly(ethylene glycol) (M_n = 5010, PDI = 1.1), 1.2 equiv of 4-pentynoic acid, DCC and 1 equiv of DMAP relative to the end group. The crude product was purified by precipitation in cold dry diethyl ether and dried in vacuo to give **12** as a solid polymer (3.54 g, 87%, T_m = 56 °C, M_n = 5290, PDI = 1.1). IR (cm^{-1}): 1738 ($O{-}C{=}O$ stretch); 1099 (C−O stretch). ^1H NMR ($CDCl_3$, 250 MHz, δ_H, ppm): 1.96 (t, 2.5 Hz, 1H, $H{-}C{\equiv}$); 2.4−2.6 (m, 4H, $-OC{-}CH_2{-}CH_2{-}C{\equiv}$); 3.35 (s, 3H, $-OCH_3$) ; 3.4−3.8 (m, $O{-}CH_2{-}CH_2{-}O$); 4.23 (t, 4.8 Hz, 2H, $-COO{-}CH_2{-}$).

Click Reaction of 2 with 10 and 13. 2 (49.8 mg, 0.25 mmol) and **10** (62.8 mg, 0.27 mmol) were dissolved in H_2O/THF (50/50, 25 mL), aqueous $CuSO_4$ (0.21 mL, 1 M, 0.21 mmol) and sodium ascorbate (0.43 mL, 1 M, 0.43 mmol) were added, and the reaction mixture was stirred at RT overnight. THF was removed in vacuo, and the residue was dissolved in CH_2Cl_2, extracted with brine, H_2O, dried with $MgSO_4$, filtered, and concentrated in vacuo. The crude product contained a minor residue of starting material that could be removed by column chromatography (EtOAc/heptane); the product was a colorless oil (77.7 mg, 72%). IR (cm^{-1}): 3112 (C−H stretch); 1756 ($O{-}C{=}O$ stretch); 1190, 1140, 1106 (C−F stretch). ^1H NMR ($CDCl_3$, 250 MHz, δ_H, ppm): 2.87 (m, 2H, ${\equiv}C{-}CH_2{-}$); 3.08 (m, 2H, $-CH_2{-}COO{-}$); 3.84 (dd, 12 Hz, 6.2 Hz, 1H, $-CH_2{-}N$); 4.26 (dd, 12 Hz, 1.9 Hz, 1H, $-CH_2{-}N$); 4.4−4.7 (m, 5H, $-CH_2{-}O$, $-CH{-}O$, $CH_2{-}CF_2$); 6.37/6.39 (2 × d, ^4J = 3.7 Hz, 2H, S−CH); 7.47 (s, 1H, $N{-}CH{=}C$).

General Procedure for Click Reaction of Polymers 3, 4, 5, 6, 7, 8, and 9 with 11 To Give Respectively 14, 15, 16, 17, 18, 19, and 20. 11 (2.2 mg, 5.7 μmol) was dissolved in DMF (0.2 mL) and mixed with a solution of $CuSO_4$ (10 μL, 0.1 M, 1 μmol) and sodium ascorbate (20 μL, 0.1 M, 2 μmol) in DMF (0.1 mL). The reaction mixture was placed on the surface of **3** and left there for 20 h. The surface was rinsed with H_2O and DMF and finally dried with pressurized air. The films were reoxidized by immersion in 10 mL of 10% Baytron C in water (~4 wt % Fe(III)Tos) in 5 min, followed by rinsing with H_2O and drying with pressurized air.

Click Reaction of 3 and 10, 21. The product was prepared according to the general click procedure on **3** using **10**(4.0 mg, 17.4 μmol), $CuSO_4$ (10 μL, 0.1 M, 1 μmol), and sodium ascorbate (20 μL, 0.1 M, 2 μmol) in DMF for 20 h.

Scheme 1. Monomer Synthesis

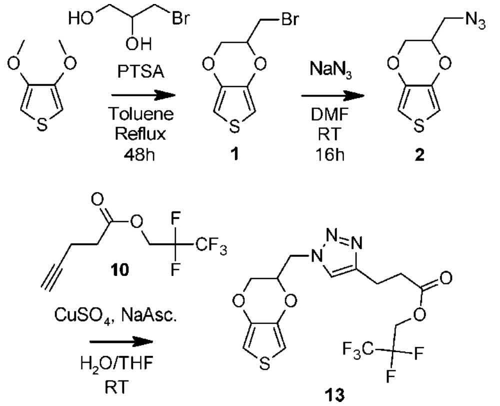

Scheme 2. Polymerization of the Azide Functional Monomer 2

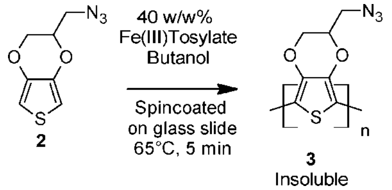

Click Reaction of 3 and 12, 22. The product was prepared according to the general click procedure on **3**, using **12**(12.3 mg, 2.4 μmol), $CuSO_4$ (10 μL, 0.1 M, 1 μmol), and sodium ascorbate (20 μL, 0.1 M, 2 μmol) in DMF or H_2O for 20 h.

Results and Discussion

In order to prepare a PEDOT for use in the click approach, it was necessary to synthesize either an alkyne or an azide functional monomer based on 3,4-ethylenedioxythiophene (EDOT). It was decided to prepare the azide monomer, since that was expected to be able to withstand the polymerization conditions. The new monomer was synthesized as shown in Scheme 1. A transetherification using 3-bromo-1,2-propanediol gives the bromine functional monomer, **1**, and this is subsequently substituted using NaN_3 to give the product monomer EDOT-N_3, **2**. The reactivity of the monomer was checked in a model reaction using standard click conditions and gave the expected product, **13**.

The polymerization method published earlier[33] was not efficient with this new monomer that appears to have a lower reactivity compared to ordinary EDOT. The polymerization rate under standard conditions is limited by pyridine. However, by omitting pyridine from the mixture, the polymerization of EDOT-N_3 occurred under otherwise similar conditions as shown in Scheme 2.

The prepared polymer is insoluble and thus cannot be characterized using NMR or SEC. However, surface characterization using XPS gives a good correlation between the expected composition and the formed substrate.

To monitor the reaction on the surface, it was decided to produce a fluorescent alkyne and detect this by fluorescence microscopy/spectroscopy. Fluorescein was chosen as precursor since it is an inexpensive fluorophore and has a high quantum yield, even after modification of the phenol and the acid group. It was expected that only a surface layer would be functionalized, and this would be difficult to detect with other techniques. In addition to this, the UV/vis spectrum of fluorescein could also be used to estimate the degree of reaction at higher concentrations.

The alkyne functional fluorophore was synthesized as shown in Scheme 3. First the methyl ester of fluorescein was prepared through an ester synthesis in accordance with the method by Moore et al.[32] In the second step the alkyne was introduced using a Mitsunobu ether synthesis in moderate yields, 48%.

At first the approach was to perform the click reactions on the polymer in H_2O with a catalyst system of $CuSO_4$ and sodium ascorbate. To make the fluorophore water-soluble, it was attempted to deprotect **11** by the method of Balakirev et al.[34] in order to perform the click reactions in water. This approach was ineffective and was abandoned. The solvent was replaced by DMF, and the catalyst system of $CuSO_4$/sodium ascorbate was applied together with **11**, which was much more efficient as shown in Scheme 4.

A reference reaction was performed without the $CuSO_4$ catalyst but with otherwise equivalent conditions. Fluorescent microscopy images of the clicked surface and the reference surface are presented in Figure 1. The distinct fluorescence of the clicked surface clearly shows that the reaction has proceeded, while the low fluorescence level of the nonclicked reference surface suggests that physical adsorption of the fluorescent reactant can be disregarded.

Fluorescent microscopy was performed on a pristine film of **11** spin-coated on a glass slide (not shown) and compared to the clicked sample. The detected fluorescence from **11** was significantly stronger than the clicked sample. This can be attributed to a combination of incomplete surface coupling and fluorescence quenching by the conducting polymer backbone. Ramanaviciene et al.[35] report that the conducting polymer polypyrrole significantly quenches fluorescein and rhodamine B fluorescence. A similar behavior was observed when a thin layer of **11** was deposited on a PEDOT-N_3 film.

The thickness of the clicked film and a reference film exposed to the same conditions except $CuSO_4$ was measured with a mechanical profilometer before and several days after the reaction. The thickness of the clicked film increased from 240 to 420 nm (±10 nm), corresponding to an increase of 75%. The thickness of the reference film was approximately unchanged by the exposure to the reaction mixture without $CuSO_4$, and a thickness of 235 nm before and 220 nm after the exposure was found. The significant volume expansion of the clicked film shows that the reaction not only is limited to the surface layer but also is occurring in the bulk phase. In addition to this the unchanged thickness of the reference film shows that the increase in thickness cannot be due to swelling or adhered reagents. The topography of the clicked sample (**14**) was investigated by atomic force microscopy (AFM) as shown in Figure 2. The surface is relatively uniform even after the large increase in thickness, and the roughness is only a few nanometers. This clearly shows that the reaction has been conducted evenly across the polymer film surface and that reactions in the bulk did not give rise to topographic differences on the surface.

X-ray photoelectron spectroscopy (XPS) was additionally used to investigate the clicked surfaces. The high-resolution peak of nitrogen shown in Figure 3 can be used to check for remaining azides on the surface due to the difference in binding energies of nitrogen in the triazole and the azide. The azide nitrogens exist in two different oxidation states resulting in two XPS peaks, one at 405 eV and one at 400 eV in a ratio of 1:2, whereas the triazole should give only one peak at 400 eV. The ratio of the two peaks in PEDOT-N_3 shown in Figure 3 is between 1:3 and 1:4. This deviation is a result of degradation of the azides during the XPS analysis. The analyses were generally undertaken with electron charge compensation to avoid charging of the less conductive film samples. XPS analysis without electron charge compensation on the highly conductive pure PEDOT-N_3 showed a constant peak ratio of exactly 1:2 for extensive analysis times, followed by an immediate decrease

Scheme 3. Fluorophore Synthesis

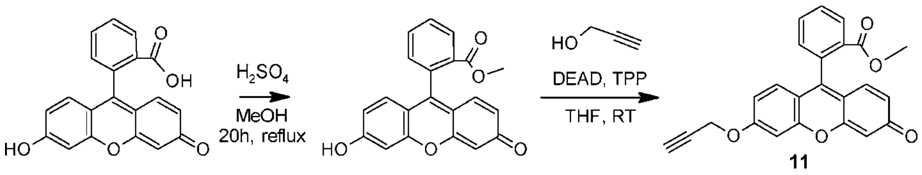

Scheme 4. Schematic of the Film Reaction of 3 with 11, Where R Substitutes 11[a]

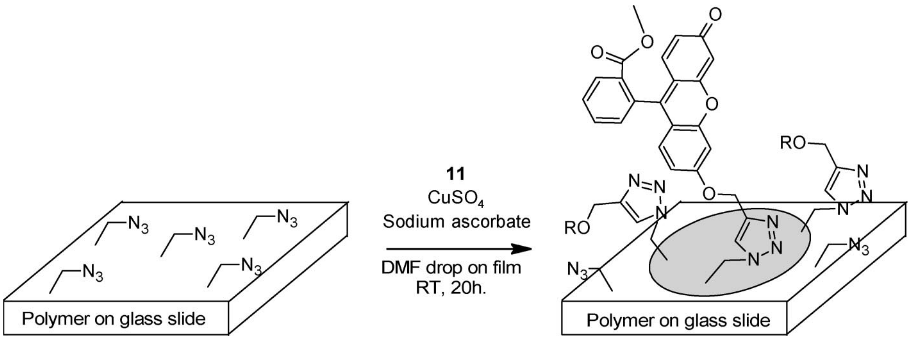

[a] The gray area indicates where the film has been exposed to the reaction mixture and thus also that there are unreacted azides around this area.

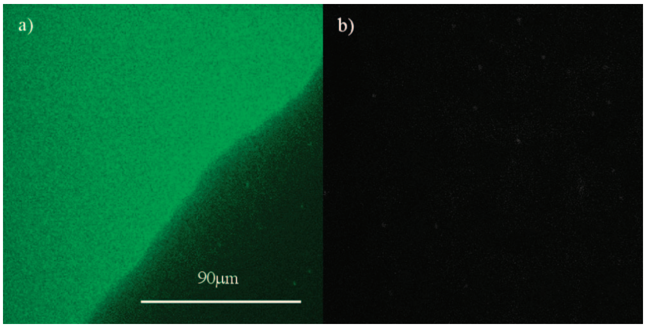

Figure 1. Fluorescence microscopy of the (a) clicked surface (**14**) and (b) the reference prepared without $CuSO_4$ under otherwise equivalent conditions. The drop of the reaction mixture did not cover the lower right corner in (a), and thus this part of the film has not been functionalized. The images are recorded using equal lighting and camera settings.

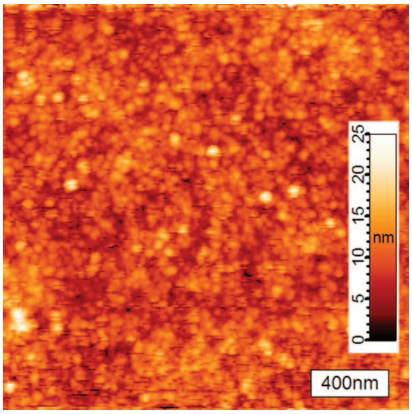

Figure 2. AFM topography image of the clicked surface of **14**.

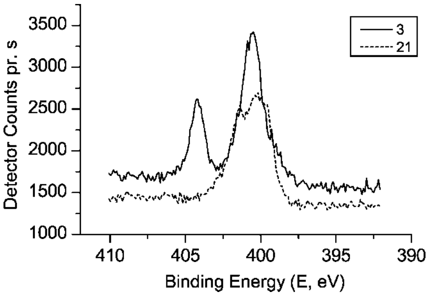

Figure 3. N (1s) high-resolution peak for PEDOT-N_3 (**3**) and the product triazole (**21**).

Table 1. XPS Results of PEDOT-N_3 (3) and the Triazoles 21 and 22 (All Numbers in atom %)

	theoretical **3**[a]	**3**[b]	**3**[c]	**21**	**22**, DMF	**22**, H_2O
C	56	61.5 (58.7)	62.0	59.5	64.4	63.2
O	18	19.5 (18.4)	20.9	17.5	26.6	21.1
N	18	9.3 (13.6)	8.6	6.7	4.6	8.4
S	8	9.6 (9.1)	8.5	5.7	4.5	7.3
F				10.6		

[a] Inclusive 33% tosylate from reoxidation based on XPS analysis of pure PEDOT films showing tosylate to EDOT ratios of approximately 1:3 in oxidized conductive films. [b] Reference sample, PEDOT-N_3 without any further treatment. Quantification in parentheses refer to analysis without electron charge compensation. [c] Reference sample, PEDOT-N_3 exposed to equivalent reaction conditions except that $CuSO_4$ was omitted.

in ratio to below 1:3 after switching on charge compensation. The relative nitrogen content also decreases with analysis time (see Table 1, second column), where especially the intensity of the peak at 405 eV is weakened. This deviation from the 1:2 ratio is in agreement with the results obtained by Shannon et al.[19] The XPS results clearly show the difference in binding energies from PEDOT-N_3 to the product triazole, where no residual azide was detected. The absence of azide nitrogens thus shows that the reaction has proceeded, though it cannot be concluded that all azides have reacted, since nonreacted azides could be degraded during the analysis. In combination with the data from the model reaction, fluorescence spectroscopy, thickness measurements, and UV/vis data (examples given in Figures 4, 5, and 8), this clearly shows that the click reaction has been performed on the polymer substrate.

The conductivity of the films is not surprisingly affected by the treatment. Before reaction the conductivity of the films is around 60 S/cm. During the reaction the films are reduced with sodium ascorbate, causing a dramatic reduction in conductivity to around 0.2−0.3 S/cm. Some of the conductivity is however regained by reoxidation in an aqueous solution of Fe(III) tosylate ending at ~15 S/cm. The actual loss in film conductance is

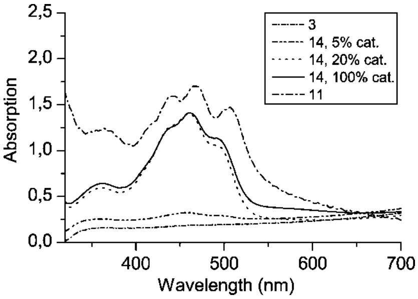

Figure 4. UV/vis spectroscopy of the fluorophore (**11**) loading on PEDOT-N_3 (**3**) as effect of catalyst concentration using a constant reaction time of 20 h.

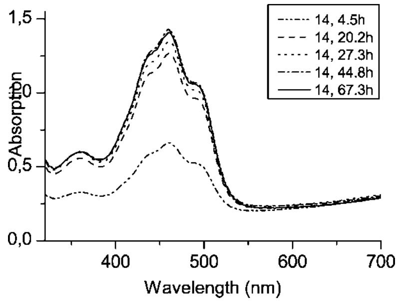

Figure 5. UV/vis spectroscopy of the fluorophore (**11**) loading on PEDOT-N_3 (**3**) as a function of reaction time using a constant catalyst loading of 20%.

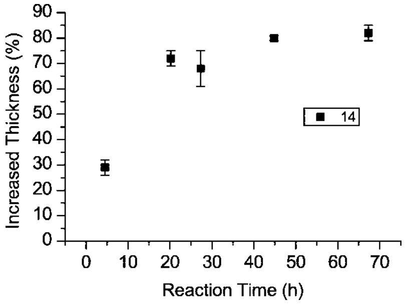

Figure 6. Increased thickness of the triazole functional polymer (**14**) as a function of reaction time using a constant catalyst loading of 20%.

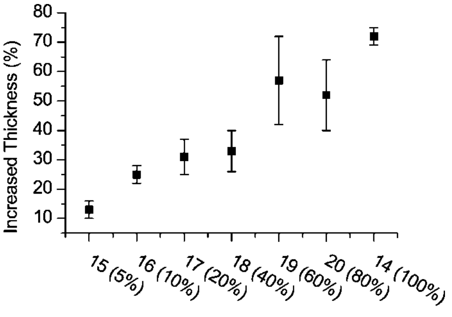

Figure 7. Increase in thickness by the click reaction as a function of EDOT-N_3 content in the copolymer.

considerably smaller than the reduction in conductivity, since the film thickness is increased by 75% after the click reaction, which in its own effect gives a reduction in conductivity.

Mechanical stirring is not possible with the polymer film, and all mixing of reagents is thus dependent on diffusion. Therefore, the necessary catalyst concentration within reasonable time frames was investigated. UV/vis spectroscopy of the films produced with a catalyst amount of 5, 20, and 100% catalyst relative to the alkyne (**11**) is presented in Figure 4 and compared to a thin layer of **11** spin-coated on a glass slide. The UV/vis spectrum shows that the 20% and 100% samples have the same three characteristic peaks as **11**, although they are blue-shifted by 5−10 nm. The strong absorption peaks supports the assumption that more than a surface layer of fluorescein is present after the reaction.

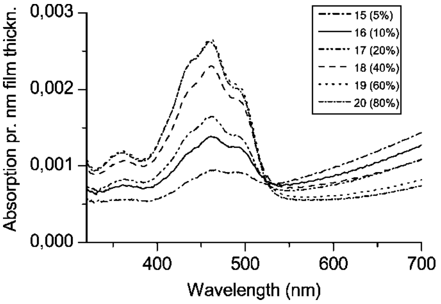

Figure 8. UV/vis absorptions per nm film thickness of the clicked copolymers, **15**−**20**.

The UV/vis absorption of the three fluorescein peaks reaches a maximum already at 20% catalyst, and conducting the reaction with 100% catalyst made no significant difference. Two explanations for this result seem feasible. Either 20% is sufficient, given the diffusion, to make the reaction proceed to completion within reasonable time or the concentration of azides is lower than assumed and all reactive sites can be initialized with 20% of the alkynes. The concentration of azides on the surface estimated based on the film thickness, film size, and the density of PEDOT that gives approximately 0.1−0.2 mg/cm^2 of azide polymer. In addition to this, access to all the azides in the film must be limited by sterical hindrance and diffusion into the polymer film, and it is expected that some of the sites may be inaccessible.

Using 20% catalyst loading the reaction time was monitored using UV/vis as shown in Figure 5. The reaction proceeds mainly within the first 20 h, and then the increase in intensity gradually decreases over time. This rate decrease is believed to be due to steric hindrance in the bulk of the polymer film as the loading increases and less free sites are available for reaction. It would demand unreasonable long reaction times to obtain complete reaction of all azides, and thus the loading obtained after 20 h has been found sufficiently high.

Film thickness measurements by profilometry corroborate these results (see Figure 6) by showing a slow progression toward larger film thickness for reactions occurring over several days.

The results from polymer films of pure EDOT-N_3 show a very high density of accessible reactive sites. Many applications may benefit from a lower density of sites with controllable average spacing, e.g., uses targeting the immobilization of large biomolecules as sensors or cellular stimulants. In order to be able to load the surface with a lower amount of azides, the copolymerization of EDOT and EDOT-N_3 was investigated. As mentioned earlier, EDOT-N_3 was less reactive than EDOT and thus polymerized without pyridine. In the copolymer formulation mixture it was necessary to include some pyridine in order to limit the EDOT polymerization since that would otherwise be too fast. It was decided to simply mix the reaction mixtures for homopolymerization of the two monomers in the ratio desired of the copolymer. This is a tradeoff as polymerization has to be slowed down sufficiently to control the EDOT reactivity without inhibiting the polymerization of EDOT-N_3 completely. The reaction was performed as shown in Scheme 5, and as with the homopolymer the product is insoluble and cannot be characterized using NMR or SEC.

Scheme 5. Copolymerization of EDOT-N_3 (2) and EDOT[a]

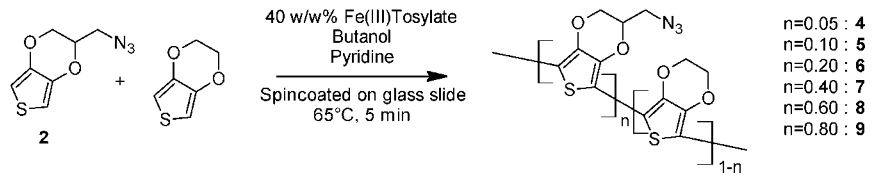

[a] Pyridine was added with EDOT to inhibit the polymerization.

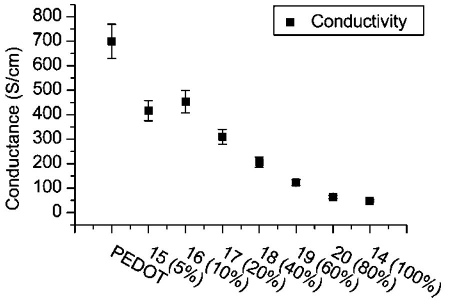

Figure 9. Conductivity of the clicked copolymers, **15**−**20**, compared to PEDOT.

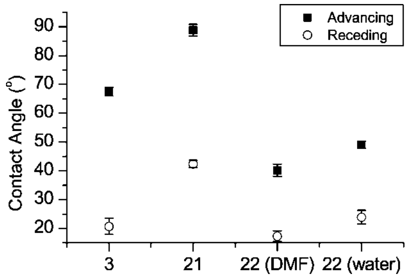

Figure 10. Contact angles of H_2O with the fluorous (**21**) and MPEG-functionalized triazole (**22**, reaction in DMF or aqueous environment) compared to the starting material PEDOT-N_3 (**3**).

Film thickness analysis of the copolymer films by profilometry revealed that increasing EDOT-N_3 content and decreasing pyridine content led to thicker polymer films. An explanation could be that more EDOT-N_3 remains after spin-coating and subsequent heating of the monomers as EDOT-N_3 is less volatile or simply that lower pyridine concentration gives less inhibition. If a specific film thickness was desired, it would have to be optimized for every ratio of the monomers in the copolymer. Since our interest in the copolymers are merely in creating a controllable density of reactive groups in the polymer, this has not been investigated further. Functionalization of the copolymers with **11** using equivalent reaction conditions was performed. As mentioned, the copolymer films are of different thickness, and thus the increased thickness by the click reaction was investigated as shown in Figure 7.

The increase in thickness was found to be dependent on the EDOT-N_3 content, which indicates that the reaction is conducted on the bulk film. This has been corroborated with fluorescence spectroscopy performed on the backside of the films which shows fluorescence. The degree of loading was also investigated using UV/vis spectroscopy as shown in Figure 8. To eliminate the effects of different film thicknesses, the results were recalculated and the relative absorbance per nm was plotted.

The corrected data clearly show that an increasing amount of reactive groups can be obtained using the copolymer approach. Interestingly, an upper degree of loading seems to be reached with 60% EDOT-N_3.

The effect on conductivity with the varied loading of the copolymer was simultaneously investigated, as shown in Figure 9. As mentioned above the functional polymers have a lower conductivity than pure PEDOT, and it is clear that the conductivity decreases with decreasing contents of EDOT. Consequently, the gain in functionality is balanced by a loss in conductivity.

To show that the method can be used as a general method for PEDOT functionalization, 2,2,3,3,3-pentafluoropropyl pent-4-ynoate, **10**, and an alkyne-functionalized MPEG 5000, **12**, were prepared. Both alkynes were produced through an ester synthesis using DCC in 88% and 87% yield, respectively. The fluorous and MPEG-functionalized polymers, **21** and **22,** have no special UV/vis absorptions that could be used to confirm the reaction. However, the changes in the surface energy properties of the PEDOT-N_3 after reaction are substantial, as can be seen from the water contact angle measurements shown in Figure 10.

It is known that introduction of fluorous compounds on a surface will decrease the surface energy and make the surface more hydrophobic.[36] By attaching the fluorous **10** to the conductive polymer, there was a distinct increase in both the advancing and receding contact angle by ~20°, which clearly shows that the reaction has proceeded and a more hydrophobic surface has been formed. The contact angle hysteresis is ~50°, indicating substantial chemical heterogeneity at the surface. It would normally be expected to obtain a higher advancing contact angle on a fluorous surface like **21**, but the effects from the tosylate ions that were introduced into the polymer through the reoxidation are believed to affect the surface oppositely. Covalent attachment of poly(ethylene glycol) entities to PEDOT-N_3 is expected to increase its surface energy, resulting in lower water contact angles. Immobilization of MPEG 5000 on the surface in **22** yields the expected lowering of the advancing contact angle by 20°−25°, depending on using either H_2O or DMF as solvent. The receding contact angle shows no significant development in either solvent compared to the untreated PEDOT-N_3. This is again consistent with a chemically heterogeneous surface, where the PEDOT/tosylate base polymer presents more hydrophilic functionalities amidst the PEG chains.

Profilometry measurements on these samples showed that the reaction performed in DMF increased the thickness by ~130 nm, corresponding to 60% for the fluorous hydrocarbon, **21**, and 60 nm corresponding to 30% for the MPEG functionalized polymer prepared in DMF, **22**. **22** prepared in H_2O had approximately the same thickness in the product as in the starting material.

XPS analysis of the clicked surfaces corroborates the results found by contact angle and by thickness goniometry and profilometry, as shown in Table 1. As mentioned earlier, the quantifications are deviating due to degradation of the azides in the sample during the analysis. However, the relative differences between PEDOT-N_3 (**3**) and the respective products can still be used for qualitative assessments. Reaction of **3** with **10** to give **21** introduced 10.6% fluorine to the surface layer, and the high-resolution nitrogen peak shows no residual azide. Thereby the reaction is confirmed, though the extent of reaction cannot be conclusively determined. The results with MPEG coupling to give **22** also correlate well with the contact angle measurements, where there is clearly a higher loading of MPEG with DMF as solvent compared to H_2O. The high-resolution peak of nitrogen shows in both cases residual azide nitrogen (not shown), which would be expected since diffusion of the long MPEG chains of **12** into the PEDOT-N_3 is much more difficult than with the smaller **10**. Regarding the MPEG experiments, the reaction is much more likely to occur only in the upper surface or perhaps only on the surface. However, there is an increased loading in the case of DMF compared to water. One may speculate that this is due to water being inefficient in swelling and wetting the PEDOT-N_3 surface. Access to reactive groups would be limited to the azides on the actual surface; thus, after reaction of about one layer of MPEG the reaction would stop. The higher loading observed with MPEG reactions in DMF could be an effect of better wetting and swelling of the surface, which would give access to an increased number of reactive sites.

Conclusion

We have developed the synthesis of a new azide monomer, EDOT-N_3, and demonstrated that it can be polymerized to PEDOT-N_3, which can be used as a precursor to obtain conductive polymers with different functionalities. A click reaction with a fluorescein derivative has been performed on the surface, and the reaction conditions have been optimized for other applications. It is possible to copolymerize EDOT-N_3 and EDOT in different ratios and to functionalize these after polymerization. Through the copolymer it is possible to control the number of reactive sites on the surface, in case a lower loading is desirable. The copolymers have also been shown to be a good way to obtain functional conductive polymers while minimizing the loss in conductivity.

By coupling the fluorous alkyne and the MPEG alkyne to the surface, we have shown the versatility of the method. We believe that this method can be applied for other alkynes with different functional groups. The approach is well suited for new sensor devices, and we are currently working on the development of different systems.

Acknowledgment. The Danish Research Council for Technology and Production Sciences (through the framework program “Design and Processing of Polymers for Microfluidic Applications”, grant 26-04-0074) is thanked for financial support.

References and Notes

(1) Dai, L. M.; Soundarrajan, P.; Kim, T. *Pure Appl. Chem.* **2002**, *74*, 1753–1772.
(2) Mateiu, R.; Lillemose, M.; Hansen, T. S.; Boisen, A.; Geschke, O. *Microelectron. Eng.* **2007**, *84*, 1270–1273.
(3) Goetzberger, A.; Hebling, C.; Schock, H. W. *Mater. Sci. Eng., R* **2003**, *40*, 1–46.
(4) Hung, L. S.; Chen, C. H. *Mater. Sci. Eng., R* **2002**, *39*, 143–222.
(5) Kolb, H. C.; Finn, M. G.; Sharpless, K. B. *Angew. Chem., Int. Ed.* **2001**, *40*, 2004–2021.
(6) Rostovtsev, V. V.; Green, L. G.; Fokin, V. V.; Sharpless, K. B. *Angew. Chem., Int. Ed.* **2002**, *41*, 2596–2599.
(7) Tornoe, C. W.; Christensen, C.; Meldal, M. *J. Org. Chem.* **2002**, *67*, 3057–3064.
(8) Lutz, J. F.; Borner, H. G.; Weichenhan, K. *Macromol. Rapid Commun.* **2005**, *26*, 514–518.
(9) Opsteen, J. A.; van Hest, J. C. M. *Chem. Commun.* **2005**, 57–59.
(10) Sumerlin, B. S.; Tsarevsky, N. V.; Louche, G.; Lee, R. Y.; Matyjaszewski, K. *Macromolecules* **2005**, *38*, 7540–7545.
(11) Helms, B.; Mynar, J L.; Hawker, C. J.; Frechet, J. M. J. *J. Am. Chem. Soc.* **2004**, *126*, 15020–15021.
(12) Parrish, B.; Breitenkamp, R. B.; Emrick, T. *J. Am. Chem. Soc.* **2005**, *127*, 7404–7410.
(13) Diaz, D. D.; Punna, S.; Holzer, P.; Mcpherson, A. K.; Sharpless, K. B.; Fokin, V. V.; Finn, M. G. *J. Polym. Sci., Part A: Polym. Chem.* **2004**, *42*, 4392–4403.
(14) Li, H. M.; Cheng, F. O.; Duft, A. M.; Adronov, A. *J. Am. Chem. Soc.* **2005**, *127*, 14518–14524.
(15) Collman, J. P.; Devaraj, N. K.; Chidsey, C. E. D. *Langmuir* **2004**, *20*, 1051–1053.
(16) Zirbs, R.; Kienberger, F.; Hinterdorfer, P.; Binder, W. H. *Langmuir* **2005**, *21*, 8414–8421.
(17) Chen, G. J.; Tao, L.; Mantovani, G.; Ladmiral, V.; Burt, D. P.; Macpherson, J. V.; Haddleton, D. M. *Soft Matter* **2007**, *3*, 732–739.
(18) Gallant, N. D.; Lavery, K. A.; Amis, E. J.; Becker, M. L. *Adv. Mater.* **2007**, *19*, 965–969.
(19) Prakash, S.; Long, T. M.; Selby, J. C.; Moore, J. S.; Shannon, M. A. *Anal. Chem.* **2007**, *79*, 1661–1667.
(20) Nandivada, H.; Chen, H. Y.; Bondarenko, L.; Lahann, J. *Angew. Chem., Int. Ed.* **2006**, *45*, 3360–3363.
(21) Brennan, J. L.; Hatzakis, N. S.; Tshikhudo, T. R.; Dirvianskyte, N.; Razumas, V.; Patkar, S.; Vind, J.; Svendsen, A.; Nolte, R. J. M.; Rowan, A. E.; Brust, M. *Bioconjugate Chem.* **2006**, *17*, 1373–1375.
(22) Binder, W. H.; Sachsenhofer, R. *Macromol. Rapid Commun.* **2007**, *28*, 15–54.
(23) Groenendaal, B. L.; Jonas, F.; Freitag, D.; Pielartzik, H.; Reynolds, J. R. *Adv. Mater.* **2000**, *12*, 481–494.
(24) Ahuja, T.; Mir, I. A.; Kumar, D.; Rajesh, *Biomaterials* **2007**, *28*, 791–805.
(25) Rahman, M. A.; Park, D. S.; Chang, S. C.; Mcneil, C. J.; Shim, Y. B. *Biosens. Bioelectron.* **2006**, *21*, 1116–1124.
(26) Higgins, S. J.; Mouffoukand, F. Patent WO2006018643-A2, **2006**.
(27) Hansen, T. S.; West, K.; Hassager, O.; Larsen, N. B. *Adv. Mater.* **2007**, *19*, 3261–3265.
(28) Hansen, T. S.; West, K.; Hassager, O.; Larsen, N. B. *J. Micromech. Microeng.* **2007**, *17*, 860–866.
(29) Hansen, T. S.; West, K.; Hassager, O.; Larsen, N. B. *Synth. Met.* **2006**, *156*, 1203–1207.
(30) Hansen, T. S.; West, K.; Hassager, O.; Larsen, N. B. *Adv. Funct. Mater.* **2007**, *17*, 3069–3074.
(31) Thomsen, A. D.; Malmstrom, E.; Hvilsted, S. *J. Polym. Sci., Part A: Polym. Chem.* **2006**, *44*, 6360–6377.
(32) Adamczyk, M.; Grote, J.; Moore, J. A. *Bioconjugate Chem.* **1999**, *10*, 544–547.
(33) Winther-Jensen, B.; Breiby, D. W.; West, K. *Synth. Met.* **2005**, *152*, 1–4.
(34) Mugherli, L.; Burchak, O. N.; Chatelain, F.; Balakirev, M. Y. *Bioorg. Med. Chem. Lett.* **2006**, *16*, 4488–4491.
(35) Ramanavicius, A.; Kurilcik, N.; Jursenas, S.; Finkelsteinas, A.; Ramanaviciene, A. *Biosens. Bioelectron.* **2007**, *23*, 499–505.
(36) Borkar, S.; Jankova, K.; Siesler, H. W.; Hvilsted, S. *Macromolecules* **2004**, *37*, 788–794.

MA702731K